Acta Crystallographica Section D
Biological Crystallography
ISSN 0907-4449

Differential effects of short affinity tags on the crystallization of *Pyrococcus furiosus* maltodextrin-binding protein

Matthew H. Bucher, Artem G. Evdokimov and David S. Waugh*

Protein Engineering Section, Macromolecular Crystallography Laboratory, Center for Cancer Research, National Cancer Institute at Frederick, PO Box B, Frederick, MD 21702, USA

Correspondence e-mail: waughd@ncifcrf.gov

Received 29 August 2001
Accepted 10 December 2001

PDB Reference: *P. furiosus* maltodextrin-binding protein in complex with maltotriose, 1elj, reljsf.

Pyrococcus furiosus maltodextrin-binding protein readily forms large orthorhombic crystals that diffract to high resolution. This protein was used as a model system to investigate the influence of five short affinity tags (His_6, Arg_5, Strep tag II, FLAG tag and the biotin acceptor peptide) on the formation of protein crystals and their ability to diffract X-rays. The results indicate that the amino-acid sequence of the tag can have a profound effect on both of these parameters. Consequently, the ability to obtain diffracting crystals of a particular protein may depend as much on which affinity tag is selected as it does on whether an affinity tag is used at all.

1. Introduction

The availability of complete genome sequences is beginning to have a profound impact on structural biology. For the first time, it is possible to select targets from among many thousands of open reading frames, any of which can easily be retrieved from its genome through the power of the polymerase chain reaction (PCR). Understandably, this perspective has conjured up visions of structural biology on a grand scale, creating a new field that has come to be known as 'structural genomics' (Burley, 2000; Blundell & Mizuguchi, 2000), but transforming this dream into reality will require technical advances that increase the speed with which the three-dimensional structures of biological macromolecules can be determined.

A generally acknowledged bottleneck in structural genomics is the production of recombinant proteins on a large scale and in a suitable form for structural studies (Christendat *et al.*, 2000). It is difficult to imagine any strategy for high-throughput protein expression and purification that does not involve the use of genetically engineered affinity tags. In addition to their obvious utility for protein purification, affinity tags have also been observed to improve the yield of recombinant proteins, help protect them from intracellular proteolysis and enhance their solubility (LaVallie & McCoy, 1995; Makrides, 1996; Nilsson *et al.*, 1997; Kapust & Waugh, 1999; Baneyx, 1999). However, a serious drawback of affinity tags is that they have the potential to interfere with the biological activity of the target protein and may impede its crystallization. This is especially true of large tags such as glutathione S-transferase (GST) and maltose-binding protein (MBP), which are among the most popular fusion partners. Diffracting crystals of MBP, GST or thioredoxin fusion proteins have been obtained in only a few instances (Kuge *et al.*, 1997; Stoll *et al.*, 1998; Center *et al.*, 1998; Liu *et al.*, 2001) and structures have been reported in just two cases (PDB code

1mg1; Kobe *et al.*, 1999; PDB code 1hsj; Liu *et al.*, 2001). Considering the prevalence of these tags in modern crystallography labs and the phasing power they could offer, it seems likely that many unsuccessful attempts to obtain crystals of fusion proteins have gone unreported. Although most fusion proteins are designed to be cleaved by site-specific proteolysis, this step often proves to be problematic and additional effort is required to separate the free target protein from the affinity tag and the protease.

Intuitively, small affinity tags (*i.e.* peptides) seem less apt to interfere with the crystallization of proteins. Indeed, more than 100 crystal structures of proteins with a hexahistidine tag (His tag; His_6) on one of their termini have been deposited in the RCSB Protein Data Bank (PDB) to date (Berman *et al.*, 2000). It seems reasonable to conclude, therefore, that the His tag is not intrinsically detrimental to the formation of protein crystals. But what about other small affinity tags? Because the structures of only a few proteins with small tags other than His_6 have been deposited in the PDB, it is not possible to draw any general conclusions about the influence of these tags on the formation of protein crystals. To gain some insight into this issue, we constructed variants of *P. furiosus* maltodextrin-binding protein (*Pfu*MBP) with five different carboxyl-terminal affinity tags (Table 1) and compared both their propensity to crystallize and the ability of the resulting crystals to diffract X-rays under rigorously controlled experimental conditions.

2. Materials and methods

2.1. Construction of *Pfu*MBP expression vectors

To construct expression vectors encoding *Pfu*MBP with either an Arg_5, His_6, FLAG, Strep II or biotin acceptor peptide (BAP) affinity tag on its C-terminus, the *Pfu*MBP open reading frame (ORF) was amplified by PCR from pKM820, which was created by inserting the ~1200 bp *Nde*I/*Bam*HI fragment of pKM800 (Evdokimov *et al.*, 2001) into the T7 expression vector pET11d (Studier *et al.*, 1990). The same N-terminal oligodeoxyribonucleotide primer (5′-GGG GAC AAG TTT GTA CAA AAA AGC AGG CTT TAA GAA GGA GAT ATA CAT ATG AAA ATC GAA G-3′) was used to construct all five *Pfu*MBP expression vectors. The C-terminal primers were: Arg_5, 5′-GGG GAC CAC TTT GTA CAA GAA AGC TGG GTT ATT AGC GAC GGC GAC GAC GTC CTT GCA TGT TGT TAA GGA TTT CTT G-3′; His_6, 5′-CAG CCT GGA TCC ATT AGT GAT GAT GGT GGT GAT GTC CTT GCA TGT TGT TAA GGA TTT C-3′; FLAG, 5′-GGG GAC CAC TTT GTA CAA GAA AGC TGG GTT ATT ATT TAT CAT CAT CAT CTT TAT AAT CTC CTT GCA TGT TGT TAA GGA TTT CTT G-3′; Strep II, 5′-GGG GAC CAC TTT GTA CAA GAA AGC TGG GTT ATT ATT TCT CAA ACT GGG GAT GAG ACC ATC CTT GCA TGT TGT TAA GGA TTT CTT G-3′; BAP, 5′-GGG GAC CAC TTT GTA CAA GAA AGC TGG GTT ATT AGT GCC ATT CGA TTT TCT GAG CTT CGA AAA TAT CGT TCA GTC CTT GCA TGT TGT TAA GGA TTT CTT G-3′.

Table 1
Short affinity tags.

Tag	Length	Sequence	Ligand
Arg_5	5	RRRRR	Cation-exchange resin
His_6	6	HHHHHH	Ni–NTA
FLAG	8	DYKDDDDK	Anti-FLAG mAb
Strep II	8	WSHPQFEK	Streptavidin
BAP	13	LNDIFEAQKIEWH	Avidin/streptavidin

The PCR products were inserted by recombinational cloning into pDONR201 (Invitrogen) to create the corresponding entry vectors. After the nucleotide sequences of the modified *Pfu*MBP ORFs were confirmed experimentally, they were moved by recombinational cloning into the destination vector pDEST14 (Invitrogen) to create the corresponding T7 expression vectors.

2.2. Protein expression and purification

The *Pfu*MBPs with C-terminal affinity tags were expressed in *Escherichia coli* BL21(DE3)-RIL cells (Stratagene). Single antibiotic resistant colonies were used to inoculate 100 ml of Luria broth (Miller, 1972) supplemented with 100 μg ml^{-1} ampicillin and 30 μg ml^{-1} chloramphenicol. These cultures were grown with shaking (225 rev min^{-1}) to saturation overnight at 310 K and then diluted 66-fold into several litres of fresh medium. When the cells reached early log phase (OD_{600nm} = 0.3–0.5), the temperature was reduced to 303 K and isopropyl-β-D-thiogalactopyranoside (IPTG) was added to a final concentration of 1 m*M*. 4 h later, the cells were recovered by centrifugation at 5000*g* for 10 min and stored at 193 K.

5 g of *E. coli* cell paste was suspended in 50 ml amylose chromatography buffer (20 m*M* Tris–HCl pH 7.4, 200 m*M* NaCl). Phenylmethylsulfonyl fluoride, ethylenediamine tetraacetic acid (EDTA) and benzamidine were added to 1, 2 and 2.5 m*M* concentrations, respectively. The cells were lysed with an APV Gaulin Model G1000 homogenizer at 69 MPa. Polyethyleneimine (PEI) was added to a final concentration of 0.1% and the lysate was then centrifuged at 37 000*g* for 10 min. Solid ammonium sulfate was slowly added to the supernatant until it reached 35% saturation. After the salt had dissolved, the mixture was clarified by centrifugation as described above. More ammonium sulfate was added to the supernatant until it reached 75% saturation and the sample was again clarified by centrifugation. The pellet was resuspended in 50 ml amylose chromatography buffer, passed through a 0.45 μm cellulose acetate membrane and then loaded onto an amylose affinity column (New England Biolabs) equilibrated with amylose chromatography buffer. The column was washed extensively with amylose chromatography buffer before the protein was eluted with 1 m*M* maltotriose in the same buffer. The peak fractions containing *Pfu*MBP were pooled and combined with an equal volume of 20 m*M* Tris–HCl pH 7.4 in order to increase the affinity of the protein for Q-Sepharose. The pooled fractions were loaded onto a Q-Sepharose column (Amersham Pharmacia Biotech)

and washed with five column volumes of 20 m*M* Tris–HCl pH 7.4, 100 m*M* NaCl. The *Pfu*MBP was eluted with a linear gradient of 100–750 m*M* NaCl over 15 column volumes. The peak fractions were concentrated by diafiltration and applied to a Sephacryl S-200 size-exclusion column (Amersham Pharmacia Biotech) equilibrated with 20 m*M* HEPES pH 8.0, 30 m*M* NaCl. The fractions corresponding to monomeric *Pfu*MBP were pooled and concentrated by diafiltration to 8–12 mg ml^{-1} for crystallization trials.

2.3. Crystallization

All *Pfu*MBP crystals were grown by hanging-drop crystallization in VDX 24-well plates containing 1 ml of precipitant solution in each well. The initial crystallization conditions for wild-type (untagged) *Pfu*MBP in complex with maltotriose were 2.3–2.5 *M* ammonium sulfate, 0.1 *M* bicine pH 9.0 (Evdokimov *et al.*, 2001). The composition of the hanging drops played an important role in the development of large protein crystals. Drop combinations ranging from 6:1 µl to 4:3 µl (protein:precipitant) were found to produce good *Pfu*MBP/maltotriose complex crystals. Large single crystals were observed in wells with drop combinations containing the highest protein-to-precipitant ratio. The crystal trays were incubated at a constant temperature of 292 K. The first crystals usually appeared after 1 d and reached their maximum size in 3–5 d.

Streak-seeding tests were performed in the following manner. A fresh well containing seed crystals was opened and the protein crystals were ground up in the drops using a blunt-end MicroTool (Hampton Research). A single dog hair glued to the end of a toothpick was used to transfer small amounts of mother liquor from the seed drop into the test drops. Each time, the tip of the whisker was washed in distilled water and wiped clean before immersion into the seed drop to ensure that the seeds were fresh and that no transfer of liquid from the target drop to the seed would occur. The target drops were resealed and incubated for several weeks at 292 K.

2.4. X-ray data collection

X-ray data collection and reduction procedures were very similar to those described previously (Evdokimov *et al.*, 2001). All the crystals used in this study could be flash-frozen in Paratone-N oil except for the *Pfu*MBP-Arg_5/maltotriose crystals, which diffracted very poorly when frozen in oil and had to be soaked in 25% sucrose in order to obtain useful data. Crystals of the *Pfu*MBP-BAP/maltotriose complex were sufficiently protected by the low molecular weight PEG in the crystallization solution and did not require additional cryoprotection, although better data were obtained using the oil.

Single crystals of the *Pfu*MBP/maltotriose complexes measuring 0.3–1.0 mm in the largest dimension were cryoprotected as described above, mounted in a monofilament loop and flash-frozen in a cryogenic nitrogen stream (Oxford Cryosystems Cryostream) at 100 K. X-ray diffraction was recorded using a MAR 345 image plate mounted on a Rigaku X-ray generator (Cu $K\alpha$ radiation) and, in the case of the *Pfu*MBP-BAP/maltotriose complex, also using an ADSC Quantum-4 CCD detector at the National Synchrotron Light Source X-9B beamline (radiation monochromated to 0.93 Å wavelength). For the data collected at home, a crystal-to-detector distance of 100 mm and an exposure time of 30 min $^{\circ -1}$ were used to collect data over 90–120° in 0.25° oscillations. For the synchrotron data, the crystal-to-detector distance was 90 mm and the data were collected in two passes using 4 and 1 min $^{\circ -1}$ for the high- and low-resolution passes, respectively. Data were collected in 0.25° oscillations covering a total of 130°, then reduced and scaled using *HKL* software (Otwinowski & Minor, 1997).

The structure of the *Pfu*MBP-BAP/maltotriose complex (crystal form *R*3) was solved by molecular replacement with the program *AMoRe* (Navaza, 1994) using the protein and carbohydrate coordinates of the native complex (1elj; Evdokimov *et al.*, 2001) and refined with *SHELXL*97 (Sheldrick & Schneider, 1997). The visible BAP-tag residues were manually built into the difference electron density using the program *O* (Jones *et al.*, 1991). The details of this 1.2 Å structure will be described elsewhere (Evdokimov *et al.*, in preparation).

3. Results and discussion

3.1. Short affinity tags

A wide variety of affinity tags have been described in the literature (reviewed by Stevens, 2000). Among the smallest are the His tag (His_6), the Arg tag (Arg_5), the FLAG tag, the Strep tag II and the biotin acceptor peptide (BAP) (Table 1). The His tag, which has been used extensively by the structural biology community, binds very tightly ($K_d \simeq 10^{-13}$ *M*) to immobilized divalent cations (*e.g.* Ni^{2+}, Cu^{2+}, Zn^{2+}; Hochuli *et al.*, 1988). A His-tagged protein can be eluted from Ni–NTA agarose by reducing the pH to ~4.5, by stripping the bound metal ions from the column with a chelating agent or with an imidazole gradient. The principle of the Arg tag is that it should endow even an acidic protein with the ability to bind to a cation-exchange column in 100–200m*M* NaCl at alkaline pH (>8.0; Sassenfeld & Brewer, 1984). Under these conditions, the vast majority of endogenous proteins will pass through the column. The Arg-tagged protein is subsequently eluted with a salt gradient. The FLAG-tag epitope is recognized by several monoclonal antibodies that can be purchased as conjugated resins (Brizzard *et al.*, 1994). Elution can be effected by calcium chelation with ethyleneglycol-bis-(β-aminoethyl ether) (EGTA) (M1 antibody only), by competitive displacement with a FLAG peptide or by transiently reducing the pH to 2.0. The Strep tag II binds relatively tightly to streptavidin ($K_d \simeq 72$ µ*M*), but not to the closely related protein avidin (Schmidt *et al.*, 1996). Biotin is a competitive inhibitor of the Strep tag II/streptavidin interaction and therefore the tagged protein can be displaced from immobilized streptavidin by biotin or its more weakly binding analogs. The BAP is an artificial substrate for the enzyme biotin holoenzyme synthetase (BirA) in *E. coli*, which catalyzes the covalent addition of biotin to the ε-amino group of a unique lysine side chain

within the peptide (Schatz, 1993). Like biotin itself, the biotinylated BAP tag is bound extremely tightly by avidin and streptavidin ($K_d \simeq 10^{-15}$ *M*; Green, 1975) and so chemically (Morag *et al.*, 1996), physically (Kohanski & Lane, 1990) or genetically (Sano & Cantor, 1995) altered forms of these proteins with weaker affinity for biotin ($K_d \simeq 10^{-8}$–10^{-9}) are usually employed for affinity chromatography.

3.2. Protein expression and purification

The impact of these five short affinity tags on the formation of protein crystals and their ability to diffract X-rays was assessed in the context of a model protein that exemplifies an ideal case. *P. furiosus* maltodextrin-binding protein readily forms large orthorhombic crystals ($P2_12_12_1$) that diffract to high resolution (Evdokimov *et al.*, 2001). Importantly, the C-terminus of *Pfu*MBP does not engage in crystal contacts in the $P2_12_12_1$ lattice and there is sufficient space between neighboring molecules to accommodate all of the tags (Fig. 1). Hence, any impact that these affinity tags might have on the formation and/or quality of $P2_12_12_1$ crystals would be unlikely to result from steric effects on crystal packing. Moreover, if any of the tags could be shown to have no effect on either parameter in the context of this model protein, this would suggest that they are not intrinsically detrimental to crystallization. The five peptide affinity tags (Table 1) were added to the C-terminus of *Pfu*MBP by using PCR to modify the expression vector. All of the *Pfu*MBP variants were expressed at a high level and in a soluble form, as observed previously for the native protein (Evdokimov *et al.*, 2001).

A major shortcoming of anecdotal reports about the negative impact of affinity tags on the crystallization of proteins is that the purification protocol is invariably altered after the tag is removed. Consequently, it is not possible to distinguish between the effect of removing the tag and the effect of changing the purification protocol. To avoid this potential pitfall, all of the *Pfu*MBP variants were purified in exactly the same fashion, without exploiting their C-terminal affinity tags. Briefly, the procedure entailed bulk fractionation with PEI and ammonium sulfate, followed by amylose affinity chromatography, ion-exchange chromatography and gel filtration. All *Pfu*MBP variants behaved similarly during purification. The final preparations were judged to be greater than 95% pure by SDS–PAGE and the molecular weights were confirmed by LC-electrospray mass spectrometry.

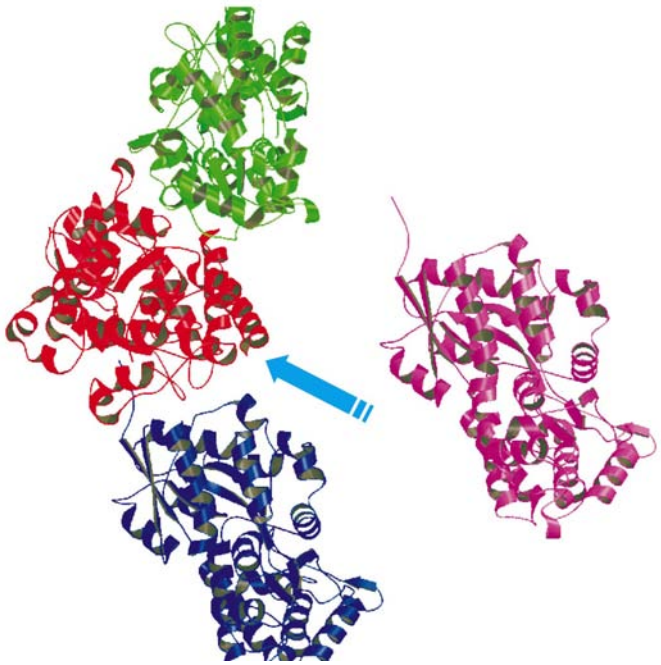

Figure 1
Packing of *Pfu*MBP in the orthorhombic crystal. The ribbon model of the reference molecule is shown in red, with an arrow pointing at its carboxy-terminus. Only those symmetry-related monomers that come within 25 Å of the five C-terminal residues of the reference molecule are shown (blue, green and magenta).

3.3. Crystallization and data collection

Initially, we attempted to obtain crystals of the affinity-tagged *Pfu*MBPs under the optimal conditions for crystallization of the untagged protein: 2.3–2.6 *M* ammonium sulfate and 0.1 *M* bicine pH 9.0. Like untagged *Pfu*MBP, the

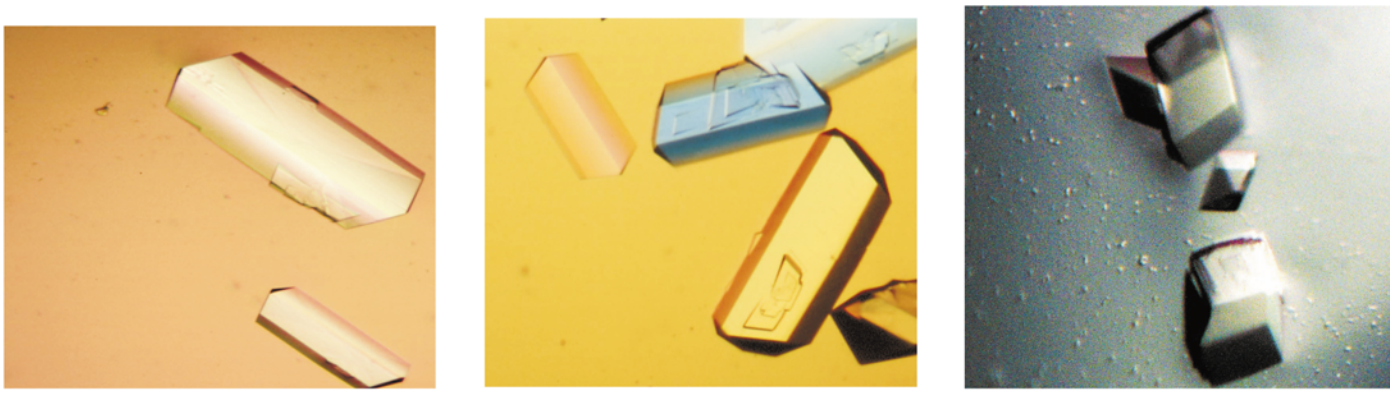

Figure 2
Microphotographs of selected *Pfu*MBP crystals. (*a*) Orthorhombic crystals ($P2_12_12_1$) of native (untagged) *Pfu*MBP. (*b*) Orthorhombic crystals ($P2_12_12_1$) of *Pfu*MBP-Arg. (*c*) Trigonal crystals ($R3$) of *Pfu*MBP-BAP.

*Pfu*MBP-His, *Pfu*MBP-FLAG and *Pfu*MBP-Arg variants all formed large crystals under these conditions (Fig. 2). Smaller crystals of *Pfu*MBP-BAP also grew under the same conditions, but no crystals of the *Pfu*MBP-Strep II variant were obtained even after streak-seeding. Thus, it appears that the presence of the Strep tag II greatly disturbed the normal crystallization pathway of *Pfu*MBP.

A more comprehensive crystal screen, using sparse-matrix kits from Emerald BioStructures (Wizard 1 and 2) and Hampton Research (HR1 and HR2), was performed with all of the *Pfu*MBP variants to see if any of the affinity tags would promote the formation of crystals under alternate conditions. The *Pfu*MBP variants that crystallized in 2.3–2.6 *M* ammonium sulfate and bicine at pH 9 also yielded crystals under several similar conditions in these screens. The *Pfu*MBP-Strep tag II protein failed to crystallize under any conditions tested. Interestingly, however, alternative conditions were found for crystallization of the *Pfu*MBP-BAP protein. The new conditions were 20% PEG 1000, 0.1 *M* NaOAc pH 4.5, 0.2 *M* $Zn(OAc)_2$. The trigonal crystals obtained under these conditions were about the same size as the orthorhombic crystals of *Pfu*MBP-BAP that grew in ammonium sulfate and bicine at pH 9 (Fig. 2). To ensure that no crystallization conditions were missed on account of slow nucleation, streak-seeding was performed with both crystal forms as seed sources. No new crystallization conditions were found using this method.

Orthorhombic crystals of *Pfu*MBP, *Pfu*MBP-His, *Pfu*MBP-FLAG, *Pfu*MBP-Arg and both types of *Pfu*MBP-BAP crystals were cryoprotected, mounted in a monofilament loop and flash-frozen in a cryogenic nitrogen stream. X-ray diffraction data were collected with a MAR 345 image plate mounted on a Rigaku X-ray generator as described previously (Evdokimov *et al.*, 2001). The results are summarized in Table 2. At this stage, we discovered that although the *Pfu*MBP-Arg crystals were visually indistinguishable from crystals of the untagged protein, their mosaicity was much greater and they diffracted rather poorly by comparison. Crystals of *Pfu*MBP-Arg also were consistently more difficult to freeze than crystals of unmodified *Pfu*MBP and the other affinity-tagged variants. In contrast to the *Pfu*MBP-Arg crystals, the quality of the orthorhombic *Pfu*MBP-His, *Pfu*MBP-FLAG and *Pfu*MBP-BAP crystals was very similar to the crystals of untagged *Pfu*MBP.

The trigonal *Pfu*MBP-BAP crystals belonged to space group *R*3, with one molecule in the asymmetric unit. Like the orthorhombic crystals, trigonal crystals of *Pfu*MBP-BAP exhibited low mosaicity (0.2–0.3°) and diffracted to high resolution with a laboratory X-ray source. The structure was solved by molecular replacement (*AMoRe*) using the coordinates of the $P2_12_12_1$ structure of untagged *Pfu*MBP as a model. The structure of *Pfu*MBP-BAP is virtually identical to that of the untagged *Pfu*MBP determined previously (Evdokimov *et al.*, 2001). As expected, however, the arrangement of molecules in the crystal lattice is different. In the $P2_12_12_1$ crystal form the N-terminal methionine residue of one molecule contacts a hydrophobic patch on the surface of the adjacent molecule, whereas in the *R*3 crystal form the consecutive isoleucine and phenylalanine residues of the C-terminal BAP contact this same hydrophobic patch in the neighboring molecule instead. With the exception of these two residues, preliminary results suggest that the BAP is disordered in the *R*3 crystal.

Table 2
Properties of *Pfu*MBP crystals.

Data were collected with a rotating-anode X-ray generator.

*Pfu*MBP	Space group	Mosaicity (°)	Unit-cell parameters (Å)			Diffraction limit (Å)
			a	*b*	*c*	
Wild type	$P2_12_12_1$	0.3	61.14	68.86	127.82	1.9
*Pfu*MBP-His	$P2_12_12_1$	0.4	61.41	68.48	128.95	1.9
*Pfu*MBP-FLAG	$P2_12_12_1$	0.4	61.14	68.17	128.40	1.9
*Pfu*MBP-Arg	$P2_12_12_1$	1.5	61.58	68.72	126.10	2.6
*Pfu*MBP-BAP	$P2_12_12_1$	0.2	61.19	68.10	129.45	2.0
*Pfu*MBP-BAP	*R*3	0.3	115.59	115.59	76.34	1.5

4. Conclusions

The objective of this study was to investigate the influence of various C-terminal peptide affinity tags on the crystallization of *Pfu*MBP. The C-terminus of *Pfu*MBP is not involved in crystal contacts and there is sufficient space between neighboring molecules in the $P2_12_12_1$ lattice to accommodate all of the tags (Fig. 1). Consequently, the differences we observed cannot readily be attributed to steric effects on crystal packing. Our observations suggest that the amino-acid sequence of the tag can have a major effect on both the formation of crystals and their ability to diffract X-rays in the context of this model protein. For example, although the Strep tag II and FLAG tags are the same length (eight residues), the former tag prevented the formation of *Pfu*MBP crystals under all conditions tested, whereas the behavior of the variant with the latter tag was virtually identical to that of the untagged protein. Additionally, $P2_12_12_1$ crystals of the *Pfu*MBP variant with the longest tag (BAP, 13 residues) diffracted to high resolution, whereas $P2_12_12_1$ crystals of the *Pfu*MBP variant with the shortest tag (Arg_5, five residues) diffracted poorly and exhibited high mosaicity even though they were visually indistinguishable from crystals of the untagged protein. These results demonstrate that the choice of which affinity tag to use can be just as important as the decision whether or not to use a tag at all and they further suggest that changing the nature of the tag is a viable alternative to eliminating it altogether when a protein fails to crystallize.

The fact that we could obtain high-quality crystals of the BAP-tagged *Pfu*MBP under unique conditions indicates that in addition to their ability to interfere with the formation of protein crystals, sometimes affinity tags can also act to promote crystallization. This inference was drawn before, when the N-terminal affinity tag on the apical domain of *E. coli* GroEL was observed to be located in the peptide-binding site of the adjacent molecule in the crystal lattice (Buckle *et al.*, 1997). However, the conjecture that the tag facilitated the

crystallization of the minichaperone was never demonstrated experimentally.

The crystal structures of two FLAG-tagged proteins have been reported (PDB code 1cq3; Carfi *et al.*, 1999; PDB code 1br2; Dominguez *et al.*, 1998) and more than 100 structures of His-tagged proteins have been deposited in the PDB. The fact that neither of these tags had any impact on the crystallization of *Pfu*MBP reinforces the notion that they are not intrinsically detrimental to the formation of protein crystals. *Pfu*MBP-Arg_5 and *Pfu*MBP-BAP are the only proteins with these affinity tags to have been crystallized thus far. The Arg_5 tag clearly compromised the quality of the crystals, casting some doubt on its suitability for this application. On the other hand, both crystal forms of *Pfu*MBP-BAP diffracted to high resolution. Curiously, although we were unable to obtain crystals of *Pfu*MBP-Strep tag II under any conditions, a 3.0 Å structure of 2-hydroxyglutaryl-CoA dehydratase component A from *Acidaminococcus fermentans* with a C-terminal Strep tag II was recently reported (PDB code 1hux; Locher *et al.*, 2001). This conflicting result underscores the fact that more data will be needed before any general conclusions can be drawn about the influence of the Strep tag II on the formation of protein crystals.

We thank Karen Routzahn for constructing the *Pfu*MBP-His_6 expression vector.

References

Baneyx, F. (1999). *Curr. Opin. Biotechnol.* **10**, 411–421.

Berman, H. M., Westbrook, J., Feng, Z., Gilliland, G., Bhat, T. N., Weissig, H., Shindyalov, I. N. & Bourne, P. E. (2000). *Nucleic Acids Res.* **28**, 235–242.

Blundell, T. L. & Mizuguchi, K. (2000). *Prog. Biophys. Mol. Biol.* **73**, 289–295.

Brizzard, B. L., Chubet, R. G. & Vizard, D. L. (1994). *Biotechniques*, **16**, 730–735.

Buckle, A. M., Zahn, R. & Fersht, A. R. (1997). *Proc. Natl Acad. Sci. USA*, **94**, 3571–3575.

Burley, S. K. (2000). *Nature Struct. Biol.* **7**, 932–934.

Carfi, A., Smith, C. A., Smolak, P. J., McGrew, J. & Wiley, D. (1999). *Proc. Natl Acad. Sci. USA*, **96**, 12379–12383.

Center, R. J., Kobe, B., Wilson, K. A., Teh, T., Howlett, G. J., Kemp, B. E. & Poumbourios, P. (1998). *Protein Sci.* **7**, 1612–1619.

Christendat, D., Yee, A., Dharamsi, A., Kluger, Y., Gerstein, M., Arrowsmith, C. H. & Edwards, A. M. (2000). *Prog. Biophys. Mol. Biol.* **73**, 339–345.

Dominguez, R., Freyzon, Y., Trybus, K. M. & Cohen, C. (1998). *Cell*, **94**, 559–571.

Evdokimov, A. G., Anderson, D. E., Routzahn, K. M. & Waugh, D. S. (2001). *J. Mol. Biol.* **305**, 891–904.

Green, N. M. (1975). *Adv. Protein Chem.* **29**, 85–133.

Hochuli, E., Bannwarth, W., Dobeli, H., Gentz, R. & Stüber, D. (1988). *Biotechnology*, **6**, 1321–1325.

Jones, T. A., Zou, J. Y., Cowan, S. W. & Kjeldgaard, M. (1991). *Acta Cryst.* A**47**, 110–119.

Kapust, R. B. & Waugh, D. S. (1999). *Protein Sci.* **8**, 1668–1674.

Kobe, B., Center, R. J., Kemp, B. E. & Poumbourios, P. (1999). *Proc. Natl Acad. Sci. USA*, **96**, 4319–4324.

Kohanski, R. A. & Lane, M. D. (1990). *Methods Enzymol.* **184**, 194–200.

Kuge, M., Fujii, Y., Shimizu, T., Hirose, F., Matsukage, A. & Hakoshima, T. (1997). *Protein Sci.* **6**, 1783–1786.

LaVallie, E. R. & McCoy, J. M. (1995). *Curr. Opin. Biotechnol.* **6**, 501–506.

Liu, Y., Manna, A., Li, R., Martin, W. E., Murphy, R. C., Cheung, A. L. & Zhang, G. (2001). *Proc. Natl Acad. Sci. USA*, **98**, 6877–6882.

Locher, K. P., Hans, M., Yeh, A. P., Schmid, B., Buckel, W. & Rees, D. C. (2001). *J. Mol. Biol.* **307**, 297–308.

Makrides, S. (1996). *Microbiol. Rev.* **60**, 512–538.

Miller, J. H. (1972). *Experiments in Molecular Genetics.* New York: Cold Spring Harbor Press.

Morag, E., Bayer, E. A. & Wilchek, M. (1996). *Anal. Biochem.* **243**, 257–263.

Navaza, J. (1994). *Acta Cryst.* A**50**, 157–163.

Nilsson, J., Stahl, S., Lundeberg, J., Uhlen, M. & Nygren, P.-A. (1997). *Protein Expr. Purif.* **11**, 1–16.

Otwinowski, Z. & Minor, W. (1997). *Methods Enzymol.* **276**, 307–326.

Sano, T. & Cantor, C. R. (1995). *Proc. Natl Acad. Sci. USA*, **92**, 3180–3184.

Sassenfeld, H. M. & Brewer, S. J. (1984). *Biotechnology*, **2**, 76–81.

Schatz, P. J. (1993). *Biotechnology*, **11**, 1138–1143.

Schmidt, T. G. M., Koepke, J., Frank, R. & Skerra, A. (1996). *J. Mol. Biol.* **255**, 753–766.

Sheldrick, G. M. & Schneider, T. R. (1997). *Methods Enzymol.* **277**, 319–343.

Stevens, R. C. (2000). *Structure*, **8**, R177–R185.

Stoll, V. S., Manohar, A. V., Gillon, W., Macfarlane, E. L. A., Hynes, R. C. & Pai, E. F. (1998). *Protein Sci.* **7**, 1147–1155.

Studier, F. W., Rosenberg, A. H., Dunn, J. J. & Dubendorff, J. W. (1990). *Methods Enzymol.* **185**, 60–89.